J Clust Sci (2017) 28:917–935
DOI 10.1007/s10876-016-1078-8

ORIGINAL PAPER

Microwave-Assisted Green Synthesis of Gold Nanoparticles Using Olibanum Gum (Boswellia serrate) and its Catalytic Reduction of 4-Nitrophenol and Hexacyanoferrate (III) by Sodium Borohydride

Atnafu Guadie Assefa[1] · Ayal Adugna Mesfin[1] · Mulugeta Legesse Akele[1] · Addis Kokeb Alemu[1] · Bhagavanth Reddy Gangapuram[2] · Veerabhadram Guttena[2] · Madhusudhan Alle[1,2]

Received: 18 July 2016 / Published online: 3 October 2016

Abstract In this work we report straightforward, an economically viable, one-step microwave-assisted green synthesis of well stabilized gold nanoparticles (AuNPs) by reducing chloroauric acid with natural water soluble olibanum gum (Boswellia serrate). The olibanum gum acts as a dual role of reducing and capping agent for synthesis of AuNPs. The formation of AuNPs was confirmed using UV–Vis spectroscopy, Fourier transform infrared spectroscopy, X-ray diffraction, transmission electron microscopy and electron diffraction. The results indicated that the synthesized NPs were well dispersed and spherical in shape had an average diameter of 3 ± 2 nm. The reaction parameters significantly affected the formation of NPs, as the concentration of gum and irradiation time increases the formation of NPs particles increases and size of particles are reduced. In addition, it has been shown that these olibanum gum capped AuNPs functioned as effective homogeneous catalyst for the reduction of two model reactions hexacyanoferrate(III) and 4-nitrophenol by sodium borohydride. The kinetic investigations were carried out at different amount of AuNPs and different temperatures.

Keywords Gold nanoparticles · Olibanum gum · Micro wave synthesis · Catalytic reduction

✉ Veerabhadram Guttena
gvbhadram@gmail.com

✉ Madhusudhan Alle
allemadhusudhan@gmail.com

[1] Department of Chemistry, University of Gondar, P.O. Box 196, Gondar, Ethiopia

[2] Department of Chemistry, Osmania University, Hyderabad, Andhra Pradesh 500007, India

Introduction

Over the past decade, noble metal nanoparticles drew significant attentions in scientific and several technological aspect because of their unique size-dependent electronic, magnetic, optical and thermal properties that are not present in their bulk counterparts [1–5]. The transition metal nanoparticles show novel properties which have various applications in nanoscience. The metal nanoparticles are of great interest mainly because of their high surface-to-volume ratio making them attractive candidates for catalysis. Among the noble metal nanoparticles, in particular gold, have been used as catalyst to promote various chemical reactions [6, 7] due to their unique size-dependent structures and properties [8, 9]. In this paper, we reported catalytic activities of AuNPs using model reactions: (a) catalytic reduction of 4-nitrophenol (4-NP) to 4-aminophenol (4-AP) by borohydride ion and (b) catalytic electron transfer reaction between potassium hexacyanoferrate (III) and borohydride ion to potassium hexacyanoferrate (II).

The synthesis of gold nanoparticles (AuNPs) has been carried out by different physical and chemical methods viz., electrochemical reduction, photochemical reduction, sonochemical, chemical reduction [10–13], etc. Most of these methods involve the utilization of harsh reducing agents like hydrazine, sodium borohydride ($NaBH_4$), dimethyl formamide (DMF) [14–16], followed by surface modification with suitable capping agent to prevent self-aggregation, and organic solvents. All of these chemicals are highly reactive, environmentally hazardous or have biological risks. To overcome such tedious techniques and utilization of harsh reducing agents, the interest in this field has shifted towards 'green' chemistry and bioprocess approach. Hence there is a need for a biosynthesis processes to synthesis of AuNPs, with negligible quantity of hazardous waste, and consume less energy than chemical synthesis method.

Recently increasing awareness towards 'green chemistry' and other biological processes induced the interest to develop a biosynthesis route for the synthesis of AuNPs which has several advantages such as simplicity, cost effective, and biocompatible reducing and capping agents for large scale commercial production of AuNPs. Early reports cited the use of natural polymers such as chitosan and its derivative carboxymethylated chitosan (CM-chitosan) [17, 18] and several plant extracts such as coriander, banana peel [19, 20] etc. The uses of Rhodopseudomonas capsulate and Zooglea ramigera like microorganism has also been demonstrated [21, 22]. Recently, the use of plant-based exudate gums for the synthesis of AuNPs has become significant because of the nontoxic and renewable nature of the chemicals, eco-friendly aqueous medium and mild reaction conditions that are advantageous over the other environmentally toxic chemicals [23]. The synthesis of AuNPs using plant based exudate gum such as salmalia malabarica, gum acacia, gum katira and gum arabic, as both reducing and capping agent was reported [24–27].

Although, various well-established techniques for the synthesis of NPs are existing, it is necessary to develop more powerful methods of the synthesis involving simple preparation procedures. The use of microwave irradiation (MWI)

is considered as a much promising technique in the regime of NPs synthesis, since it has a more rapid volumetric heating, higher reaction rate and selectivity, short reaction time, and high yield as compared to conventional heating methods [28, 29]. Previous reports related that as compared to conventional heating, microwave irradiation creates NPs of narrower size distributions and higher degree of crystallinity and endowments, greater control over the size and shape morphology [30]. Hence, MW synthesis is quickly becoming an attractive alternative in NPs synthesis.

Olibanum gum is naturally occurring gum-oleo-resin obtained as an exudate from the bark of Boswellia serrate (Burseraceae family), a native tree of India and Ethiopia. It is easily available, non-toxic, eco-friendly, cost effective, biodegradable, and renewable polysaccharide gum [31, 32]. Besides that it is used in fumigant, infuriate and multipurpose aromatic; it also exploited in pharmaceutical, cosmetic, food, paint, textile industries and ceramic. This gum is used in traditional ayurvedic and unani medicine for the treatment of hypolipidemic, hepato-protective, reno-protective [33] and anticancer agent [34]. It is also used in a potent vaccine adjuvant [35], and as matrix for controlled release of diclofenac [36]. Typically, the gum consists of volatile oil, water soluble gum (polysaccharides), lipophilic terpenes and insoluble matter. The primary structure of this gum is made up of sugars such as galactose, arabinose, xylose and D-glucuronic acid [37–39]. Aruna Jyothi et al. synthesis of AgNPs has been carried out using olibanum gum by autoclave method [40]. To the best of our knowledge green synthesis of AuNPs using olibanum gum as reducing and stabilizing agent by MWI has not yet been reported.

The present work details a sustainable green approach to the synthesis of AuNPs using naturally occurring olibanum gum acting as a reducing and stabilizing agent and water as a solvent by MWI method. Its natural availability, non-toxicity, medical value, low cost and multifunctional nature has arisen the interest of the researchers to select this gum for the present study. The formation of AuNPs has been characterized by using UV–Vis spectroscopy, Fourier transform infrared spectroscopy (FTIR), X-ray diffraction (XRD), transmission electron microscopy (TEM) and EDX analysis. The main focus in this study is olibanum gum capped AuNPs acting as efficient catalyst for the reduction of aromatic nitrophenol to aminophenol and also the electron transfer reaction between $K_3[Fe(CN)_6]$ and $NaBH_4$. The kinetic study of the reduction of 4-NP and $K_3[Fe(CN)_6]$, catalyzed by AuNPs catalyst with variable concentrations of $NaBH_4$ and AuNPs was carried out.

Materials and Methods

Chemicals

Olibanum gum (OG) grade-1, was purchased from Arada market, Gondar, Ethiopia, Tetrachloroauric (III) acid ($HAuCl_4$) was purchased from Sigma-Aldrich (St. Louis, MO, USA), 4-Nitrophenol (4-NP), Sodium borohydride ($NaBH_4$), Potassium hexacyanoferrate (III), Nitric acid (HNO_3), Hydrochloric acid (HCl) and Sodium

hydroxide (NaOH) were obtained from Merck Limited, Mumbai, India. All these are of AR Grade. All aqueous solutions of olibanum gum, and tetrachloroauric acid were made using deionized water purified using a Mill-Q Plus system.

Synthesis of AuNPs

Glassware was cleaned in a bath of freshly prepared aquaregia solution (HCl:HNO_3 3:1) and then rinsed thoroughly with Milli-Q water. Before the preparation of AuNPs, the stock solution of 0.5 % olibanum gum (0.5 g of OG and 0.2 g of NaOH) was prepared in Milli-Q water. The solution was stirred overnight and turned into a homogeneous solution. An aqueous solution of $HAuCl_4$ (1 mL, 1 mM) was mixed with a diluted solution of 3 mL olibanum gum. The reaction mixture was stirred, then shifted into a microwave oven. The microwave oven (2.45 GHz with maximum power 300 W) used was a focused single mode microwave system (Discover, CEM, USA), which was equipped with a magnetic stirrer and a water-cooled condenser. During the heating process, the color of the reaction mixture changed slowly from light yellow to ruby red color reduction of Au^{3+} to AuNPs. The reaction mixture was analyzed by UV–Vis spectroscopy to establish the formation of AuNPs. The formation of AuNPs was investigated by varying the microwave irradiation time from 1 to 10 min, olibanum gum concentration (0.1–0.5 %), and $HAuCl_4$ concentration (0.1–1 mM). The solution of the synthesized AuNPs was centrifuged at high speed (20,000 rpm). The pellet and supernatant liquid were separated. The pellet was again dispersed in Milli-Q water.

Characterization

UV–Vis spectra of olibanum gum capped AuNPs were recorded with UV–Vis-NIR Spectrophotometer (UV-3600, Shimadzu) having a scanning range of 200–700 nm against a blank gum solution used. FTIR analysis was carried out to determine the possible functional groups of the olibanum gum, which are involved in the reduction and stabilization of synthesized NPs. The obtained colloidal solution of AuNPs was first lyophilized and then the sample was used for FTIR analysis, prepared in the form of a thin pellet with potassium bromide (KBr). A pure KBr pellet was used as a background and this was subtracted from the FTIR spectra of the olibanum gum and AuNPs sample. FTIR spectra were recorded with an instrument IR Affinity-1 (Shimadzu) in the scanning range of 650–4000 cm^{-1}. The crystallinity of the olibanum gum capped AuNPs was determined by X-ray diffractometer (De Schakel 18, 5651 GH Eindhoven, Netherlands) instrument operating at 40 kV and a current of 30 mA at a scan rate of 0.388 min^{-1}. The morphology and size distribution of the olibanum gum capped AuNPs dispersion was carried out by TEM measurement: casted nanoparticle dispersion on carbon-coated copper grid and allowed to dry at room temperature. Measurements were done on TECHNAI G2 F30 S-TWIN instrument (FEI Company, Hillsboro, OR, USA) operated at an accelerated voltage of 200 kV with a lattice resolution of 0.14 nm and point image resolution of 0.20 nm. The presence of atomic gold was determined using a scanning electron microscopy (Model: EDXA Zeiss Evo50, Carl

Zeiss AG, Germany). The sample were dried at room temperature and then analysed for composition of the synthesized NPs.

Catalytic Reduction of 4-Nitrophenol

The catalytic activity of olibanum gum capped AuNPs was studied using $NaBH_4$ reduction of 4-nitrophenol (4-NP) to 4-aminophenol (4-AP) as a unique reaction. The reaction procedure was as follows: initially freshly prepared 1 mL of 15 mM $NaBH_4$ solution was mixed with1.7 mL of 0.2 mM 4-NP solution in 3 mL volume of quartz cuvette. At this stage, the change of colour from light yellow to yellow-green was observed. Varying concentrations of (50–150 μL) of AuNPs solution was added to the above mixture. The absorption spectra were recorded on UV–Visible spectrophotometer with a time interval of 1 min and a wavelength range between 200 and 600 nm at different temperatures (25–70 °C).

Reduction of Hexacyanoferrate (III)

The catalytic activity of olibanum gum capped AuNPs in electron transfer reaction between Hexacyanoferrate (III) and $NaBH_4$ was investigated. The reaction procedure was as follows; initially 0.7 mL of 10 mM $Fe(CN)_6^{3-}$and freshly prepared 1.5 mL of 36 mM $NaBH_4$ in 0.1 M NaOH aqueous solution was mixed with 1 mL of Milli-Q water, the reaction mixture was taken in a 3 mL quartz cuvette. To this mixture varying concentrations of (50–150 μL) of AuNPs solution were added. Thus, the absorbance intensity of ferricyanide for the initial reaction was recorded at 420 nm. After the addition of AuNPs the intensity decrease was monitored by using UV–Vis spectrophotometer. The electron transfer reaction was performed at different temperatures between 25 and 70 °C.

Results and Discussion

Olibanum gum is sparingly soluble in water, the solubility of olibanum gum can be increased by converting to sodium salt of olibanum gum by the addition of specific amount of sodium hydroxide. This sodium salt of olibanum gum can act as reducing agent as well as a stabilizing agent for the formation of AuNPs which has been reported in the present work for the first time. In our synthetic procedure, this olibanum gum has a dual role as a reducing agent and capping agent. The major advantage of using microwave is the fast synthesis with controlled size of AuNPs. Furthermore, olibanum gum has been preferred as it is eco-friendly polysaccharide, easily available, and low cost that motivated the researchers in the preparation of NPs.

UV–Visible Spectroscopy Analysis

The formation of AuNPs was observed due to the Surface Plasmon Resonance (SPR) of the AuNPs by using UV–Vis spectroscopy. Theoretical studies on the

dependence of the UV–Vis absorption on the size of the metal spheres have been conducted [41]. In this study, the general trend is that the SPR absorption band showed a red shift with increasing particle size. In addition, the aggregation of colloidal gold causes a decrease in the intensity of the main peak, and also resulted in a long tail on the long-wavelength side of the peak. After microwave irradiation, the sodium salt of olibanum gum containing auric chloride solution changed its color significantly from pale yellow to blushing red, due to the reduction of Au^{3+} ions to AuNPs under reducing action of olibanum gum.

The Fig. 1a displays absorption spectra of AuNPs prepared using olibanum gum in different concentrations (0.1–0.5 %) at a fixed concentration of auric chloride (1 mM $HAuCl_4$) and MWI for 10 min. The results obtained in this examination have revealed a number of findings which can be presented briefly as: (a) the spectra exhibited characteristic SPR band located at spectral 530 nm, ascribed to the formation of AuNPs. Such result suggested that AuNPs could be successfully obtained by using alkali-stabilized olibanum gum which can reduce the Au^{3+} to AuNPs due to the –OH groups present in the gum. This –OH group mediated reduction was reported for the synthesis of AuNPs; (b) the peak position of AuNPs did not change, which clearly suggested that the particles were well dispersed without aggregation; and (c) the efficacy of formation of AuNPs increased with increase in the concentration of olibanum gum from 0.1 to 0.5 %. This may be attributed to the formation of more of AuNPs with the progress of the reaction, since the intensity of the surface plasmon peak is directly proportional to the density of the AuNPs in solution.

On the other hand Fig. 1b displays the absorption spectra of AuNPs prepared using $HAuCl_4$ in different concentrations (0.1–1 mM) at a fixed concentration of olibanum gum (0.5 %) and MWI for 10 min. The absorption spectra still showed one absorption peak located at 530 nm due to the SPR of the AuNPs and no other peak was detected in the range between 540 and 700 nm. This result clearly indicated that no aggregation occurred in this reactive system and the nanoparticles

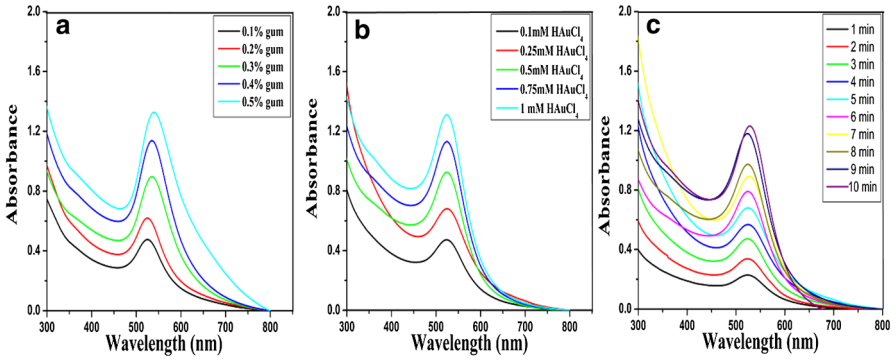

Fig. 1 UV–Vis absorption spectra of the AuNPs synthesized **a** different concentration of olibanum gum solution containing 1 mM $HAuCl_4$ by MWI 9 min, **b** different concentration of $HAuCl_4$ solution containing 0.5 % olibanum gum by MWI 9 min, **c** different concentration of 1 mM $HAuCl_4$ solution containing 0.5 % olibanum gum at different MWI time ranging from 1 to 10 min

were found to be dispersed well [42]. The efficacy of formation of AuNPs increased with increase in the concentration of $HAuCl_4$, reflecting the formation of more and more AuNPs. The prepared NPs were not bigger in size due to the capping effect of olibanum gum. Therefore, it is possible that a huge amount of AuNPs with small particle size can be achieved using olibanum gum as a capping and reducing agent.

The preparation of AuNPs was also examined by different MWI times (1–10 min) with 1 mM $HAuCl_4$ and 0.5 % olibanum gum as shown in Fig. 1c. The data in Fig. 1c revealed numerous significant findings which can be presented as follows: at the initial stage of reaction duration (i.e., <2 min), the surface plasmon band is broad and weak, indicating low conversion of gold ion to AuNPs in this irradiation duration. As the MWI time increased up to 7 min resulted in the strongest SPR band to occur at 530 nm, implying the reduction of huge amounts of gold to AuNPs. Additional increase in the MWI time to 8 min resulted in a gradual increase in the absorption intensity without any shift in the peak wavelength, signifying an increase in AuNPs content with increasing MWI time. It also showed that the mean diameter of the AuNPs did not change much. Further, raising irradiation time to 10 min was accompanied by the absorption band shifting to a longer wavelength (537 nm) which could be attributed to the expansion in the AuNPs size.

FT-IR Spectra of AuNPs

The involvement of functional groups of olibanum gum in the reduction and stabilization of AuNPs was clearly explained by using FTIR spectra. Figure 2 shows the FTIR spectra of olibanum gum and olibanum gum capped AuNPs. In the case of olibanum gum the major vibrational peaks were found to be located at 3421, 2932, 1726, 1617, 1427, 1244, and 1033 cm^{-1}. The peaks placed at around 3421 and 2932 cm^{-1} can be assigned to the stretching vibration of the O–H and C–H group. The other strong peaks observed at 1726, 1617 and 1427 cm^{-1} could be attributed

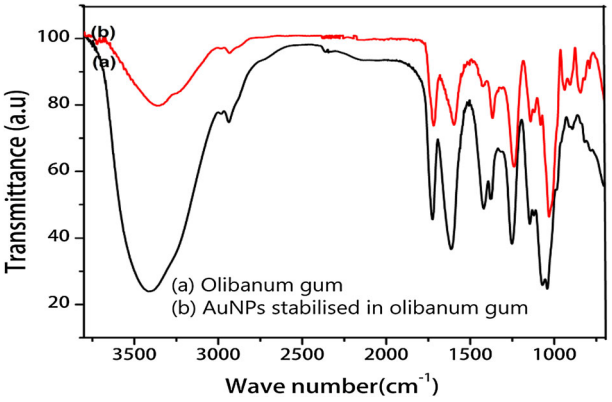

Fig. 2 FTIR anlysis of the (*a*) pure olibanum gum and (*b*) olibanum gum capped gold nanoparticles indicating the involvement of functional group in the formation of AuNPs

to characteristic asymmetrical and symmetrical stretches of the CO_2^- (carboxylate ion) group connected with the olibanum gum. The absorption bands at 1244 and 1033 cm^{-1} correspond to C–O–C stretching polymer gum molecule. The stretching vibrational frequencies of olibanum gum capped AuNPs were detected at 3356, 2932, 1719, 1595, 1448, 1259 and 1065 cm^{-1}. In the case of olibanum gum capped AuNPs, the peaks shifted from 3421 to 3356, 1726 to 1719, 1617 to 1595 and 1427 to 1438 cm^{-1} and other peaks were found to remain unchanged. These results indicated that hydroxyl groups and the carboxyl groups were involved in the synthesis and stabilization of AuNPs. The formation of AuNPs with olibanum gum acts as a dual role: as reducing agent for gold ion and as capping agent after the formation of AuNPs.

XRD Analysis of AuNPs

The XRD analysis was performed to confirm the presence of crystalline Au in the synthesized AuNPs. Figure 3 shows characteristic XRD pattern of the olibanum gum capped AuNPs prepared with 0.5 % olibanum gum and 1 mM $HAuCl_4$, and with microwave irradiated for 9 min. Four distinct characteristic peaks were observed at $2\theta = 38.25, 43.95, 64.5, 77.21$ respectively, corresponding to the (111), (200), (220), and (311) sets of lattice planes which may be indexed as the band for face-centered cubic (fcc) crystal structure of crystalline metallic Au (JCPDS No. 04-0784). The absence of extra peaks in XRD-spectrum indicated that the synthesized AuNPs are of pure crystalline. The peak corresponding to the (111) plane is most intense compared to the other peaks. The broadening of these peaks was mostly due to the effect of nano-sized particles. Crystallite size of AuNPs was calculated using the Scherrer equation together with the XRD data and was found to be around 4 ± 3 nm which is consistent with the TEM analysis (3 ± 2 nm).

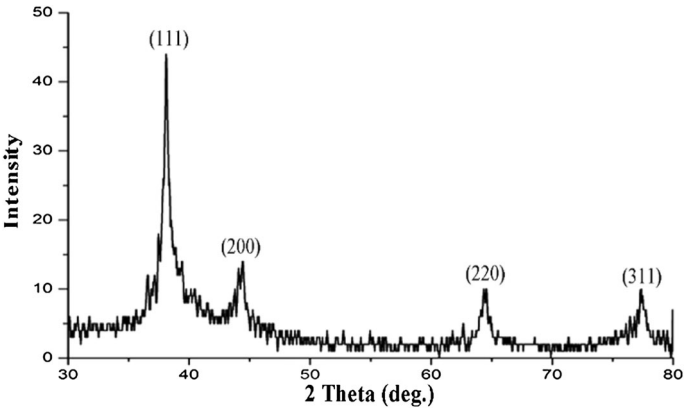

Fig. 3 XRD pattern of gold nanoparticles stabilized by olinanum gum indicating the crystalline nature of AuNPs

TEM and SAED Pattern of AuNPs

The size, shape and morphology of the sustainable green synthesized AuNPs were further determined by TEM images. Figure 4a presents the typical TEM images of the gold nanoparticles synthesized with 0.1 % olibanum gum and 1 mM $HAuCl_4$ by

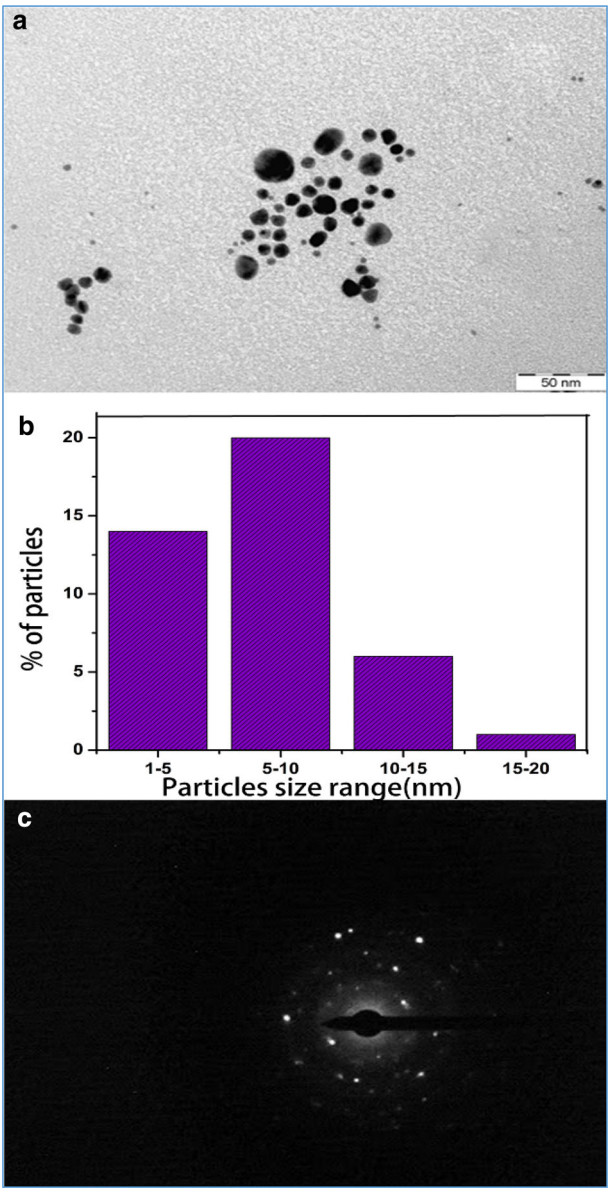

Fig. 4 TEM image of synthesized gold nanoparticles with **a** 0.5 % of olibanum gum and 1 mM of $HAuCl_4$, **b** histogram showing particle size distribution **c** corresponding SAED pattern

MWI for 5 min, which showed that most of the AuNPs obtained were spherical and uneven shaped. The particle size distribution measured for 41 NPs in TEM image across a representative sample is shown in Fig. 4b. The average particle diameter was 8 ± 4 nm. The selected-area electron diffraction (SAED) pattern, which is shown in Fig. 4c, exhibited diffuse ring pattern, indicating that these AuNPs are highly polycrystalline in nature. These four rings can be ascribed to the diffraction from the (111), (200), (220) and (311) lattice planes of face centered cubic (fcc) gold, respectively.

To know the effect of capping nature of gum extract over growth and formation of AuNPs, experiments were conducted with various concentrations (0.1 and 0.5 %) of olibanum gum with fixed concentration of precursor (1 mM $HAuCl_4$) and 9 min MWI time as shown in Fig. 5a, c. The prepared NPs were found to be spherical in shape and well dispersed in gum matrix. The average particle diameter obtained from these micrographs was about 8 ± 2 (0.1 % olibanum gum) to 3 ± 4 nm (0.5 % olibanum gum) as shown in Fig. 5b, d. These findings clearly indicated as the concentration of gum increases from 0.1 to 0.5 %, the average size of AuNPs formed decreased. These studies are analogous to a previous work on the green synthesis of silver nanoparticles with gum kondagogu and sodium alginate, in which the concentration of the gum increased from 0. 1 to 0.5 % [43, 44]. This study indicated that the particle size of the AuNPs can be controlled by using various

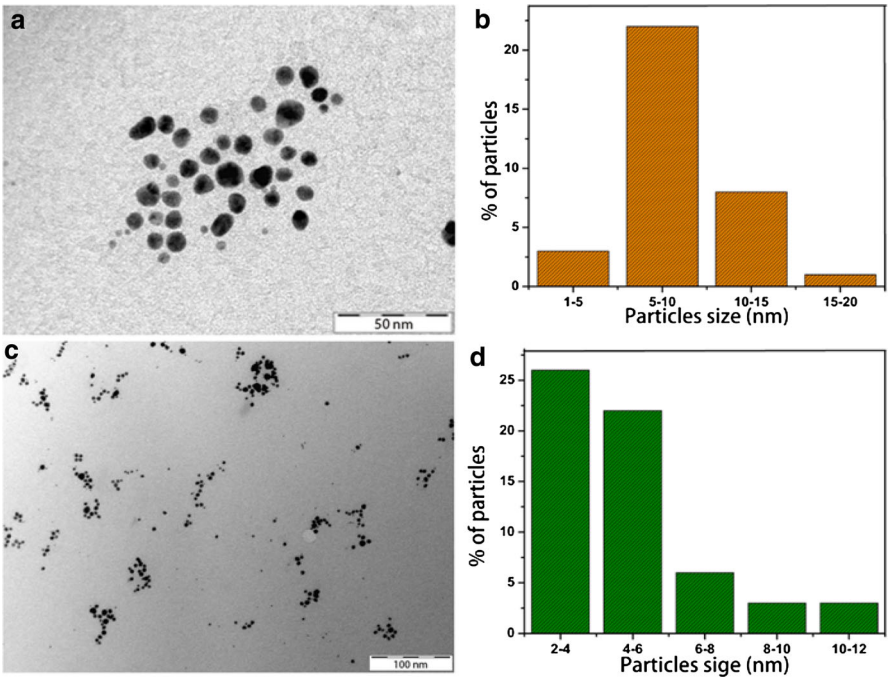

Fig. 5 TEM photo-micrographs showing **a** 0.1 % olibanum gum, of precursor (1 mM $HAuCl_4$) and 9 min MWI times. **c** 0.5 % olibanum gum, 1 mM of $HAuCl_4$ and 9 min MWI time. **b**, **d** Histograms of the particle size distribution of 0.1 and 0.5 % of gum

concentrations of gum solution. At higher concentration of gum, the interaction between gold ion and functional groups on gum, as well as the rate of nanoparticle capping were excellent. In addition, the aggregation of nanoparticles was lower due to lesser collisions of AuNPs. As the concentration of gum increased from 0.1 to 0.5 % the formation of AuNPs also increased and this finding is consistent with the UV–Vis results. As a result, nanoparticles with monodispersity were obtained with 1 mM of $HAuCl_4$, 0.5 % of olibanum gum and 9 min of MWI time.

EDX Analysis

The presence of Au atoms in the olibanum gum capped AuNPs was further confirmed by energy dispersive x-ray analysis (EDXA). The EDXA spectrum recorded in the spot profile, displayed one of the densely populated NPs region on the surface of olibanum gum. Strong peaks of Au (Fig. 6) at 2.195 keV energy that are characteristic of AuNPs along with C and O were observed which may have originate from the olibanum gum bound to the surface of the AuNPs. The appearance of Cu was due to the use of a Cu grid in EDXA analysis.

Stability Study of AuNPs

The stability of eco-friendly synthesised, olibanum gum capped AuNPs in solution is an important requirement for their chemical and biological application. This feature was studied by monitoring the SPR under different pH and electrolytic conditions over a reasonable period of time. The red shift normally observed in UV–Visible spectra is an indication of an agglomeration of NPs or increase in the size of the particle or both. The synthesized AuNPs did not show any shift in the SPR peak. The peak intensity was decreased due to the dilution with varying concentrations

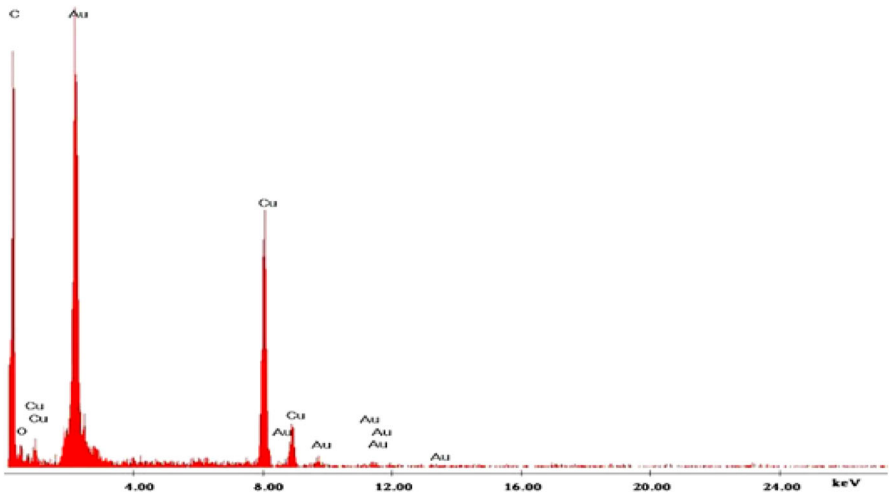

Fig. 6 EDXA analysis of gold nanoparticles synthesized with 0.5 % (w/v) olibanum gum and 1 mM $HAuCl_4$, MWI for 9 min

(1–5 M) of sodium chloride (NaCl) (Fig. 7a). Varying the pH of the solution between 2 and 9 did not also alter the size of NPs and no major agglomeration was observed (Fig. 7b). The stability of as synthesized AuNPs were stable up to 3 months at room temperature (Fig. 7c) due to the protection of olibanum gum on the nanoparticles surface.

Homogeneous Catalytic Reduction of 4-Nitrophenol

To investigate the redox catalytic activities of the synthesized AuNPs using the olibanum gum, we selected a well-known catalytic reaction for the transformation of 4-NP to 4-AP in the presence of sodium borohydride ($NaBH_4$). This reaction was monitored using UV–Visible spectroscopy. The absorption peak of 4-NP underwent red shift from 317 to 400 nm immediately after addition of $NaBH_4$, conforming the change in the colour of the solution from yellow to intense yellow. This change in colour could reveal the formation of 4-nitrophenolate ions under alkaline conditions. The peak at 400 nm remained unaltered for many days in the absence of AuNPs. This indicates the inability of $NaBH_4$ to reduce 4-NP which could be due to a very large kinetic barrier for the reduction reaction. Remarkably, on the addition of aliquot of AuNPs to nitrophenolate ion, a rapid decrease in the intensity and disappearance of the absorption peak within few minutes at 400 nm was observed. The reduction process was monitored by measuring the time-dependent absorption spectra of the reaction mixture. During this time interval, there was an appearance of a new peak of 4-AP at 300 nm, indicating the generation of reduction product 4-AP. The time-dependent UV–Visible spectra of 4-NP hydrogenation with olibanum gum capped AuNPs are shown in Fig. 8. A small peak at 530 nm indicated that there was almost no change observed in the SPR of AuNPs during the induction period and 4-NP reduction. This observation suggested that the concentration of AuNPs remained roughly constant and not changed in the course

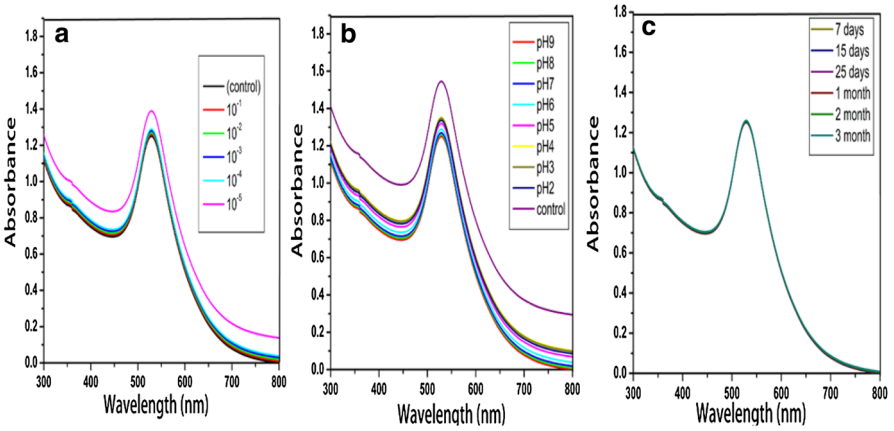

Fig. 7 UV–Vis spectra of AuNPs depicting their high stability due to the influence of olibanum gum capping. Stability of olibanum gum stabilized AuNPs were tested against **a** different electrolytic (NaCl) concentration; **b** varied pH conditions; and **c** 3 month stability study showing no aggregation

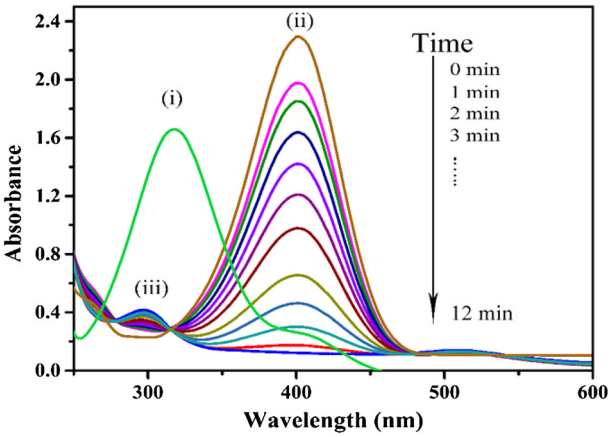

Fig. 8 Time dependent UV–Vis absorption spectra of the reduction of 0.2 mM 4-nitrophenol by 15 mM $NaBH_4$ in the presence of olibanum gum capped AuNPs (150 µl) as catalyst. (*i*) 4-NP, (*ii*) reduction of nitrophenolate ion with time interval of 1 min, (*iii*) 4-AP

of catalytic reaction, even in the presence of a higher concentration of reducing agent $NaBH_4$. From this, it can be inferred that the catalytic activity of AuNPs was a surface reaction phenomenon.

In this catalytic reduction, the initial concentration of $NaBH_4$ added to the reaction mixture far exceeded the concentration of 4-NP, and the extra BH_4^- resulted an increase in the pH of the system, thus hindering the degradation of BH_4^-. The liberated hydrogen from the reaction is purged out, thereby checking the aerial oxidation of the reduced product of 4-NP. It is believed that both 4-NP and reducing agent BH_4 are absorbed on the surface of AuNPs and the surface efficient transfer of electron (e^-) from donor BH_4^- ion to 4-nitrophenolate, mediated by the NPs, thereby dropping activation energy of the chemical reaction and increase the rate of reaction without that of 4-NP and catalyst, and it is reasonable to assume that the concentration of $NaBH_4$ remains constant during the reaction [45]. In this context, pseudo-first order kinetics could be used to evaluate the rate constant of the present catalytic reaction. The rate constant (k) was determined from the linear plot of ln (A_o/A_t) vs reaction time.

In order to examine the role of the catalyst for the reduction of 4-NP to 4-AP, the experiments were conducted by varying the amount of AuNPs (50–150 µL), while other parameters such as temperature, concentration of $NaBH_4$, and 4-NP remaining constant. Figure 9 shows the rate constant value plotted against varying amount of catalyst. As the amount of AuNPs increased the rate of reduction reaction became much faster and 400 nm peak disappear within 12 min with the formation of 4-AP. As the amount AuNPs increases the rate of the reactions also proportionally increases because the NPs lowered the activation energy of the reaction and played the role of catalyst. Thus, 150 µL of AuNPs acts as effective catalyst for the conversation of 4-NP to 4-AP.

Temperature was taken as the main parameter related to the study of rate of the reaction for the reduction of 4-NP to 4-AP and was studied in temperature range

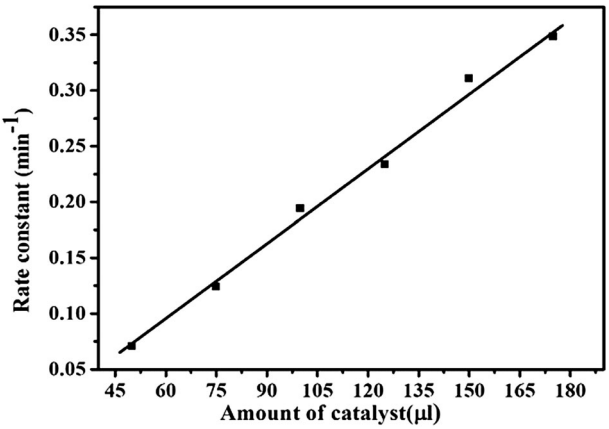

Fig. 9 Plot of the rate constant against different amount of AuNPs. The reaction conditions: 0.2 mM 4-NP; 15 mM $NaBH_4$ various amount of AuNPs obtained from different quantities of 1 mM of $HAuCl_4$ and 0.5 % olibanum gum

25–70 °C keeping other parameter constant. The activation energy was calculated from slope (E_a/RT) by linear plot of ln$k$ on l/T, using the Arrhenius equation $k = \ln A - Ea/RT$, where k can be defined at given temperature (in Kelvin) as rate constant, A is Arrhenius constant and R is universal gas constant. The catalytic reduction of 4-NP was studied at six different temperatures (25, 30, 35, 45, 55, 65 and 70 °C) using olibanum gum capped AuNPs as catalyst. Investigation of activation energy was made as a plot of ln$k$ and the reciprocal temperature. A plot of ln$k$ versus l/T, shown in Fig. 10, is a linear curve for 4-NP reduction using AuNPs. It was observed that the rate of reaction increases with increase in the temperature. Computing activation energy was performed from the graph of straight line range of

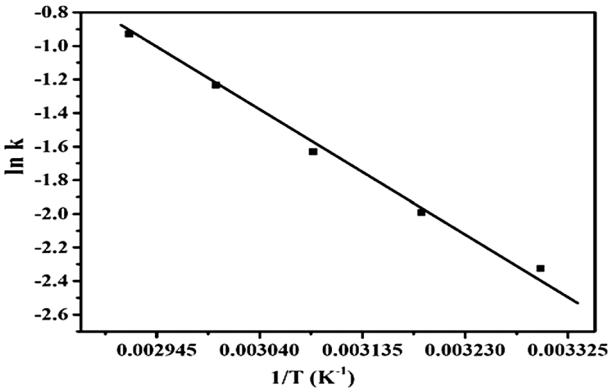

Fig. 10 Plot of rate constant against l/T for the reduction of 4-NP by $NABH_4$ in the presence of AuNPs as catalyst at different temperatures ranging from 250 to 70 °C.The concentrations of $NaBH_4$, 4-nitrophenol, and AuNPs are 15 mM, 0.2 mM, and 150 µl, respectively

ln$k$ against l/T. The value was calculated to be 7.4 ± 1.34 k Cal/mol. The above results clearly indicated that the catalytic reaction was carried out on NPs surface.

Catalytic Reduction of Potassium Hexacyanoferrate (III)

The redox couple interaction between sodium borohydride and hexacyanoferrate (III) resulted in the formation of hexacyanoferrate (II) ion and dihydrogen borate ion which was strongly catalyzed by AuNPs. The redox reaction is described as:

$$BH_4^- + 8\,[Fe(CN)_6]^{3-} + 3H_2O \rightarrow 8\,[Fe(CN)_6]^{4-} + H_2BO_3^- + 8H^+.$$

The advantage of hexacyanoferrate ion for this redox study is that both oxidation states of iron (+2 and +3) are quite stable with respect to dissociation and hydrolysis. The resulted hexacyanoferrate ions in both oxidation states of iron (+2 and +3) are much resembled to each other in terms of chemical composition and geometrical shape. The redox potential corresponding to the reaction being studied, E^o (Fe^{2+}/Fe^{3+}) is +0.44 V versus a normal hydrogen electrode (NHE). The standard reduction potential of the borate ion is $E^o = -1.24$ V. Hence, there is a huge free energy change associated with the reaction. However, this reaction can even continue in the absence of a catalyst, but it has been reported that it is a slow reaction, which follows zero-order kinetics [46].

The kinetics of the reduction reaction can be regarded as a pseudo first-order reaction because, the concentration of $NaBH_4$ was large excess as compared to hexacyanoferrate (III) ions, and the reduction rate can be assumed to be independent of $NaBH_4$ concentration. The rate of reduction reaction was monitored UV–Vis spectrum of hexacyanoferrate (III). The characteristic absorption peak of hexacyanoferrate (III), located at 420 nm remained unaltered for a long time in the absence of catalyst AuNPs, indicating the inability of the strong reducing agent $NaBH_4$ itself to reduce hexacyanoferrate (III). Interestingly, up on addition of an aliquot of AuNPs, the intensity of the absorption peak at 420 nm continuously decreased and disappeared within 23 min as shown in Fig. 11. During the redox reaction process the SPR of (530) AuNPs remained unaffected. This could be a clear evidence that the AuNPs did not aggregate during their catalytic activity. Moreover, this could also indicate that the reactants and the NPs did not undertake any chemical reaction. The kinetics of reduction reaction of hexacyanoferrate (III) catalyzed by AuNPs was studied using various amounts of catalyst and temperature ranges of 30–70 °C.

The effect of catalyst for the reduction of potassium hexacyanoferrate (III) to potassium hexacyanoferrate (II) was determined by varying the amount of AuNPs (50–250 μL), while other parameters being kept constant. Figure 12 shows the rate constant values plotted against various amounts of catalyst. The linear increase in the rate of the reaction has been observed as the amount of catalyst increases. This may be because of available reaction surfaces of the catalysts. As shown in Fig. 12, this is a linear relationship between the observed rate constant and the concentration of AuNPs.

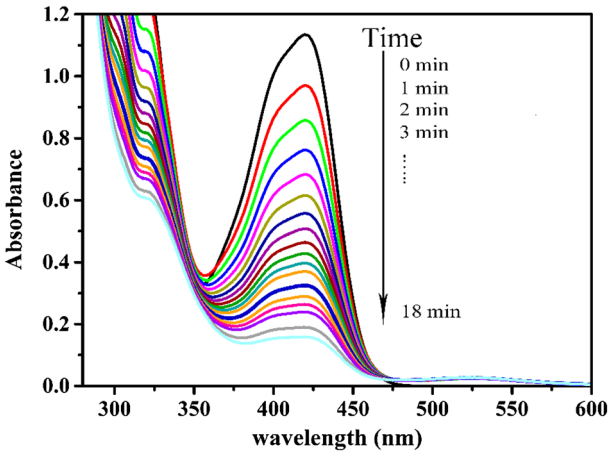

Fig. 11 Time dependent UV–Vis absorption spectra of the reduction of 10 mM hexacyanoferrate (III) by 15 mM $NaBH_4$ in the presence of olibanum gum capped AuNPs (250 µl) as catalyst

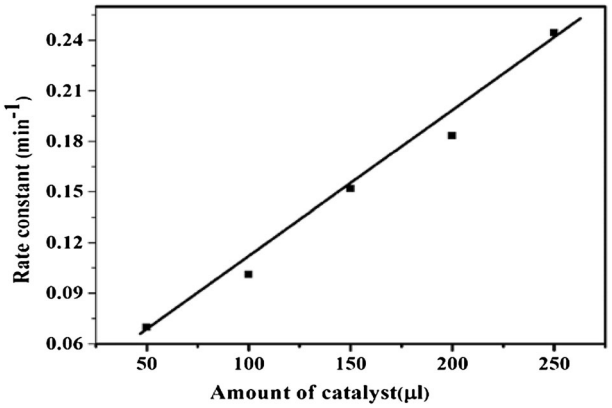

Fig. 12 Plot of rate constant against different amounts of AuNPs obtained from 1 mM of $HAuCl_4$ and 0.5 % of olibanum gum

Figure 13 shows the Arrhenius plots of the ln(k) versus 1/*T* for the reaction catalyzed by these AuNPs. In this study, the plot of the ln(k) versus 1/*T* showed Arrhenius behavior within 30–70 °C temperature range while other parameters being kept constant. Thus, the slope (−Ea/R) was used to compute the required activation energy. It was observed that increasing temperature of the reaction helped the rate of the reaction to increase. The activation energy of the reaction was found to be 7.3 k Cal/mol. The reaction rate reached a nearly constant value at the higher temperatures above 70 °C. The effect of size of AuNPs on its catalytic activity has been studied and optimized results are given in the present publication. As the size of the nanoparticles increases the catalytic activity increases due to increase in the surface area of AuNPs.

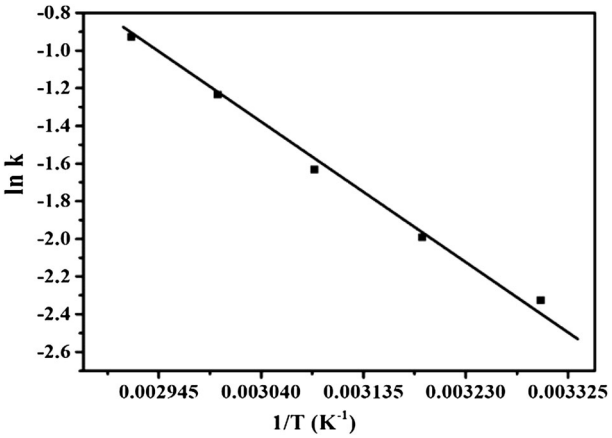

Fig. 13 Plot of rate constant against l/T for the reduction of hexacyanoferrate (III) by $NABH_4$ in the presence of AuNPs as catalyst at different temperatures

Table 1 Catalytic activity of the AuNPs for the conversation of 4-NP to 4-AP and hexacyanoferrate (III) to hexacyanoferrate (II): comparison

Catalyst	Type of NPs	Target	Size (nm)	Time (min)	Rate constant K (min^{-1})	Ref
AuNps	Spherical	4-NP	3 ± 4	12	0.35	This work
PMAA/Pd	Spherical	4-NP	25	26.4	0.1391	[47]
CuNPs	Spherical	4-NP	5.6	50	0.0952	[48]
AgNPs	Spherical	4-NP	25	15	6.7×10^{-2}	
PtNNs	Ball-shaped	$K_3[Fe(CN)_6]$	60–100	60	$(9.1 \pm 0.7) \times 10^{-3}$	[49]
PtNBs	Ball-shaped	$K_3[Fe(CN)_6]$	60–100	60	$(16.9 \pm 0.6) \times 10^{-2}$	[49]
AuNPs	Spherical	$K_3[Fe(CN)_6]$	3 ± 4	18	0.24	This work

A comparison of efficiencies of different catalysts is given in the Table 1. It has been observed that AuNPs catalyst shows higher efficiency in the conversion of p-nitrophenol to p-aminophenol and potassium hexacyanoferrate (III) to potassium hexacyanoferrate (II).

Conclusions

In this study, a simple, efficient and economically viable "green'' approach has been established for the synthesis of AuNPs. The synthesis was carried out in an aqueous medium by a microwave using olibanum gum (Boswellia serrate) as a

reducing and stabilizing agent without using any harsh, synthetic reducing agents. The greener synthesis of olibanum gum capped AuNPs was found to be eco-friendly due to the utilization of renewable plant material. The amount of gum and irradiation time affected the formation of AuNPs. The study showed that microwave irradiation can accelerate the formation of AuNPs. The study indicated that the particle size decreases with increasing concentration of gum. The synthesized olibanum gum capped AuNPs are highly stable, and have shown effective catalysis in the reduction of 4-NP to 4-AP and electron transfer reaction between $K_3[Fe(CN)_6]$ and $NaBH_4$ to form $K_4[Fe(CN)_6]$. The detailed kinetic features of catalytic reaction was evaluated by changing the reaction conditions. Increasing the amount of the catalyst and reaction temperature resulted in the rate of the reaction to increase but decrease of the reaction time. We believe that this method described above, could be extended to provide a promising route to prepare other metal nanoparticles, which could be very useful for catalytic applications.

References

1. P. Alivisatos (2004). *Nat. Biotechnol.* **22**, 47.
2. J. Dai and M. L. Bruening (2002). *Nano Lett.* **2**, 497.
3. H. Hiramatsu and F. E. Osterloh (2004). *Chem. Mater.* **16**, 2509.
4. Y. Mei, Y. Lu, F. Polzer, and M. Ballauff (2007). *Chem. Mater.* **19**, 1062.
5. X. Shi, K. Sun, and J. R. J. Baker (2008). *J. Phys. Chem. C.* **112**, 8251.
6. A. Stephen and K. Hashmi (2007). *Chem. Rev.* **107**, 3180.
7. M. C. Daniel and Didier Astruc (2004). *Chem. Rev.* **104**, 293.
8. C. Lin, K. Tao, D. Hua, Zhen Ma, and S. Zhou (2013). *Molecules* **18**, 12609.
9. H. Jans and Q. Huo (2012). *Chem. Soc. Rev.* **41**, 2849.
10. G. Sandmann, H. Dietz, and W. Plieth (2000). *J. Electroanal. Chem.* **491**, 78.
11. Y. P. Sun, P. Atorngitjawat, and M. Meziani (2001). *J. Langmuir.* **17**, 5707.
12. K. Okitsu, M. Ashokkumar, and F. Grieser (2005). *J. Phys. Chem. B.* **109**, 20673.
13. R. J. Nikhil, G. Latha, J. Catherine, and Murphy (2001). *Chem. Mater.* **13**, 2313.
14. A. Manna, P. L. Chen, H. Akiyama, T. X. Wei, K. Tamada, and W. Knoll (2003). *Chem. Mat.* **15**, 20.
15. H. Sakai, T. Kanda, H. Shibata, T. Ohkubo, and M. Abe (2006). *J. Am. Chem. Soc* **128**, 4944.
16. I. P. Santos, M. Luis, and M. Liz (1999). *Langmuir* **15**, 948.
17. H. Z. Huang, Y. Qiang, and X. R. Yang (2005). *J. Colloid Interface Sci.* **282**, 26.
18. A. Madhusudhan, G. Bhagavanth Reddy, M. Venkatesham, and G. Veerabhadram (2014). *Int. J. Mol. Sci.* **15**, 8216.
19. K. B. Narayanan and N. Sakthivel (2008). *Mater. Lett.* **62**, 4588.
20. A. Bankar, B. Joshi, A. R. Kumar, and S. Zinjarde (2010). *Colloids Surf. B.* **80**, 45.
21. S. He, Z. Guo, Y. Zhang, S. Zhang, J. Wang, and N. Gu (2007). *Mater. Lett.* **61**, 3984.
22. N. Srivastava and M. Mukhopadhyay (2015). *J. Clust. Sci.* **26**, 675.
23. S. Dhar, E. M. Reddy, A. Shiras, V. Pokharkar, and B. L. V. Prasad (2008). *Chem. Eur. J.* **14**, 10244.
24. G. Reddy, A. Madhusudhan, D. Ramakrishna, D. Ayodhya, M. Venkatesham, and G. Veerabhadram (2015). *Int. Nano. Lett.*. doi:10.1007/s40089-015-0158-3.
25. G. B. Reddy, D. Ramakrishna, A. Madhusudhan, D. Ayodhya, M. Venkatesham, and G. Veerabhadram (2015). *J. Chin. Chem. Soc.* **62**, 420.
26. S. Maity, I. K. Sen, and S. S. Islam (2012). *Physica E.* **45**, 130.
27. C. Chen Wu and D. Hwang Chen (2010). *Bulletin* **43**, 234.
28. J. F. Zhu, Y. J. Zhu, M. G. Ma, L. X. Yang, and L. Gao (2007). *J. Phys. Chem. C.* **111**, 3920.
29. M. B. Mohamed, K. M. Abou Zeid, V. Abdelsayed, A. A. Aljarash, and El-Shall (2010). *ACS Nano* **4**, 2766.
30. M. Tsuji, M. Hashimoto, Y. Nishizawa, M. Kubokawa, and T. Tsuji (2005). *Chemistry* **11**, 440.

31. C. K. Atal, B. Singh, S. Kour, S. Singh, G. B. Singh, and C. L. Gupta (1983). *Indian J Pharmacol* **15**, 35.
32. G. B. Singh, S. Bani, and S. Singh (1996). *Phytomedicine* **3**, 87.
33. R. S. Pandey, B. K. Singh, and Y. B. Tripathi (2005). *Indian J Exp Biol.* **43**, 509.
34. O. B. Choi, J. H. Park, Y. J. Lee, C. K. Lee, K. J. Won, J. Kim, et al. (2009). *J Physiol Pharmaco.* **13**, 107.
35. A. Khajuria, A. Gupta, F. Malik, S. Singh, J. Singh, B. D. Gupta, et al. (2007). *Vaccine* **25**, 4586.
36. K. P. R. Chowdary, P. Mohapatra, and M. Murali Krishna (2006). *Indian J Pharm Sci* **68**, 497.
37. P. K. Shukla, P. Bhatnagar, and R. Yadav (2005). *Vaniki Sandesh.* **29**, 23.
38. A. Upaganlawar and B. Ghule (2009). *Ethnobot Leaflets* **13**, 766.
39. A. K. Sen, A. K. Das, N. Banerji, and M. R. Vignon (1992). *Carbohydr Res.* **223**, 321.
40. K. Aruna Jyothi, R. B. Sashidharb, and J. Arunachalama (2012). *Process Biochemistry* **47**, 1516.
41. K. Anand, R. M. Gengan, A. Phulukdaree, and A. Chuturgoon (2015). *J. IND. ENG CHEM.* **21**, 1105.
42. M. Brust, M. Walker, D. Bethell, D. J. Schiffrin, and R. J. Whyman (1994). *Chem. Soc. Chem. Commun.* **7**, 801.
43. K. Aruna Jyothi, R. B. Sashidhar, and J. Arunachalam (2010). *Carbohydrate Polymers* **82**, 670.
44. X. Zhao, Y. Xia, Q. Li, X. Ma, F. Quan, C. Geng, and Z. Han (2014). *Physicochem. Eng. Aspects* **444**, 180.
45. L. Qiu, Y. Peng, B. Liu, B. Lin, Y. Peng, J. Muhammad. Malik, and F. Yan (2012). *Applied Catalysis A: General* **413**, 230.
46. S. C. Romero, J. P. Juste, P. Herves, L. M. L. Marzan, and P. Mulvaney (2010). *Langmuir* **26**, 1271.
47. S. Bi, K. Li, X. Chen, W. Fu, L. Chen, H. Sheng, and Q. Yang (2014). *Polym. Compos.*. doi:10.1002/pc.
48. D. Pangkita, C. Ramesh, Deka, and B. Pankaj (2014). *New J. Chem* **38**, 1789.
49. M. K. Ajit, K. Kiran Kumar Sharma, L. Anaïs, A. Fabrice, R. Hynd, Abhijit Saha, and K. Geeta Sharma (2013). *Langmuir* **29**, 11431.